京都大学防災研究所年報 第 55 号 B 平成 24 年 6 月
Annuals of Disas. Prev. Res. Inst., Kyoto Univ., No. 55 B, 2012

Numerical Analysis on Countermeasures of Bank Erosion in the Sesayap River

Puji HARSANTO(1), Hiroshi TAKEBAYASHI
and Masaharu FUJITA

(1) Graduate School of Engineering, Kyoto University

Synopsis

Countermeasures of the bank erosion problem considering the horizontal two dimensional flow patterns and bed deformation are discussed in this paper. Numerical analysis is performed using the horizontal two-dimensional bed deformation model which the equations are written in general coordinate system. The presence of the mid-channel bar in the river is one of the factors causes the riverbank erosion in the rivers. The results from the numerical model indicate that dredging of the mid-channel bar with the appropriate level reduces the bed degradation near the bank toe, especially at the lee area. Revetment can protect the bank directly. However, the installation of revetment makes the bank line smoother. As a result, the flow velocity to the opposite bank becomes faster and the possibility that local scouring is accelerated along the opposite bank increases.

Keywords: bank erosion, mid channel bar, numerical analysis, bed deformation

1. Introduction

In alluvial rivers, the mass failures due to geotechnical instability of the bank are one of the most common phenomena. The bed deformations near the bank toe are the substantial parameters in practical concern for channel and bank stabilization (Thorne, 1991). Many training works were applied at rivers to prevent bank erosion such as groin, revetment, spur dike and so on. Most of them are structure, which are installed on the bank body to protect mass failure or erosion on the bank surface and to improve bank stability. The structures will be successful in protecting the riverbank locally. However, usually the structures will change the cross-sectional geometry, which leads to change the flow pattern and others hydraulics parameters. In an extreme case, the structure will produce another bank erosion problem in another place, especially in case that the flow is a dominant factor in riverbank erosion problem. Study on the bank erosion problem considering the horizontal two dimensional flow patterns and bed deformations are important for achieving a successful countermeasure.

Numerical simulation is one of the methods to predict the future condition. It is useful for planning or designing in hydraulic problem. In this study, the numerical simulation was developed to analyze the future condition of the flow pattern and the bed deformation of the river regarding to the countermeasure method on the bank erosion problem. This analysis will be applied in a river in Indonesia. In Sesayap River East Kalimantan Indonesia, the presence of a huge mid-channel bar accelerates the erosion by flows. The flow that deflected around the bars is a primary cause of the bank erosion problem. To control the flow by dredging of the bars may give the significant result in a countermeasure of the riverbank erosion.

In case of riverbank erosion with the mass

failure process occurred in Sesayap River, the bed deformation near the bank is one of the input parameters to predict the bank stability. The increase in relative height of riverbank that caused by bed scour has a strong influence on the stability of riverbank. So, the bed degradation near the riverbank is one of the important data on bank stability analysis. Therefore, an analysis of bed deformation near the bank with accurate calculation is needed.

2. Outline of the Sesayap River

The Sesayap River is located in East Kalimantan Indonesia. This river passes through at Malinau city, capital of Malinau district, which established as a new district in 1999 belongs to East Kalimantan province. Total drainage area for Sesayap River system is 18.158 km^2, which small part belonged to Malaysia's territorial. The river has 279 km long. The river reach in study area is about 80 km from estuarial and still have influenced by sea tide level. The tide's characteristic is semi diurnal with a mean range of 2 m and the maximum amplitude of 3 m. Fig. 1 and Fig. 2 show the location of study area and characteristics of water level during one month.

Based on alluvial river's classification (Schumm, 1985), Sesayap River is representing a meander-braided transition channel. Sediment loads are large, and sand, gravel, and cobbles are a significant fraction of the bed load. These formations indicate the river flow have high-energy (Brierley and Fryirs, 2005). Fig. 3 shows the grain size of the bed load transport. The mid-channel bar is formed on riverbed dominantly (see in Fig. 1).

The growth of mid-channel bars may become an important factor in the bank erosion problem in this river. As bar head modifies flow direction in the river and changes flow pattern and velocity as shown in Photo 1.

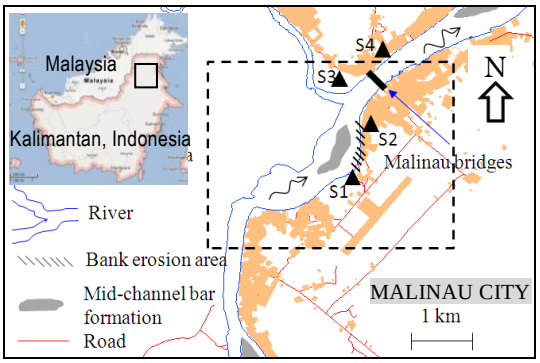

Fig. 1 Study area on Sesayap River reach in Malinau city

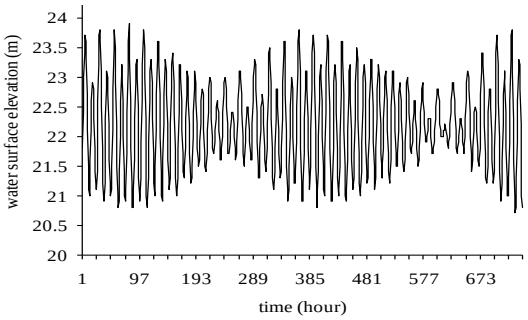

Fig. 2 Water surface elevation at downstream Sesayap River

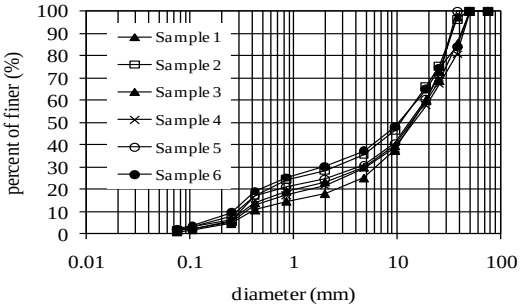

Fig. 3 Grain size of Sesayap River at Malinau

Photo 1 The head of mid-channel bars split the river flow

Photo 2 Mass failure on Sesayap riverbank

Photo 2 shows the mass failure and damages on the street. The location is near the mid channel bar (see Fig. 1). Cohesion content of the bank affects strongly on the block failure phenomena of bank (Dulal and Shimizu, 2010) and the bank erosion rate increases rapidly in case which the upper and the lower bank materials are composed of cohesive material and non-cohesive material, respectively (Takebayashi et al., 2010). Fig. 4 and Photo 3 show the typical bank stratification in study reach area. The stratification is cohesive layer lies on the non-cohesive layer. This field survey results show that the mid channel bar and bank stratification are the main factors on triggering bank erosion in this river reach.

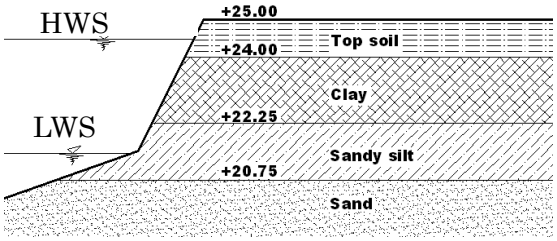

Fig. 4 Bank startification in study reach area

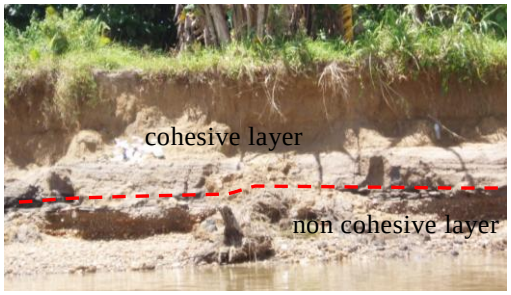

Photo 3 Stratification of Sesayap riverbank

3. Numerical Analysis

Numerical simulations for the Sesayap River are performed using the horizontal two-dimensional flow model which the equations are written in general coordinate system. To simulate the effect of the mid-channel bar dredging, the average daily discharges (Q = 434.63 m3/s) used for upstream boundary. The downstream boundary is the water surface as shown in Fig. 2 and the initial size distribution of the river bed is non-uniform as shown in Fig. 3. The calculation reach of the river is about 4.3 km long. Computation of the water flow is performed using the governing equation of the horizontal two dimensional flow averaged with depth. Relationship between Cartesian coordinate system and General coordinate system is as follows.

$$J = \frac{1}{\left(\frac{\partial x}{\partial \xi}\frac{\partial y}{\partial \eta} - \frac{\partial x}{\partial \eta}\frac{\partial y}{\partial \xi}\right)} \tag{1-1}$$

$$\frac{\partial \xi}{\partial x} = J\frac{\partial y}{\partial \eta} \tag{1-2}$$

$$\frac{\partial \eta}{\partial x} = -J\frac{\partial y}{\partial \xi} \tag{1-3}$$

$$\frac{\partial \xi}{\partial y} = -J\frac{\partial x}{\partial \eta} \tag{1-4}$$

$$\frac{\partial \eta}{\partial y} = J\frac{\partial x}{\partial \xi} \tag{1-5}$$

Where, ξ and η are the coordinates along the longitudinal and the transverse directions in the generalized coordinate system, respectively, x and y are the coordinates in Cartesian coordinate system. Computation of surface flow is carried out using the governing equation of the horizontal two-dimensional flow averaged with depth. The conservation of mass, i.e., inflow and outflow of mass by seepage flow, is taken into consideration as shown in the following equation (Takebayashi, 2005).

$$\Lambda\frac{\partial}{\partial t}\left(\frac{z}{J}\right)+\frac{\partial}{\partial \xi}\left(U\frac{h}{J}\right)+\frac{\partial}{\partial \eta}\left(V\frac{h}{J}\right)+\frac{\partial}{\partial \xi}\left(U_g\frac{h_g}{J}\right)+\frac{\partial}{\partial \eta}\left(V_g\frac{h_g}{J}\right)=0 \tag{2}$$

Where, t is the time, z is the water surface level. Surface flow depth is represented as h, seepage flow depth is h_g. U and V represent the contravariant depth averaged flow velocity on bed along ξ and η coordinates, respectively. These velocities are defined as

$$U = \frac{\partial \xi}{\partial x} u + \frac{\partial \xi}{\partial y} v \tag{3}$$

$$V = \frac{\partial \eta}{\partial x} u + \frac{\partial \eta}{\partial y} v \tag{4}$$

where, u and v represent depth averaged flow velocity on bed along x and y coordinates, respectively. U_g and V_g represent the contravariant depth averaged seepage flow velocity along ξ and η coordinates, respectively. These velocities are defined as

$$U_g = \frac{\partial \xi}{\partial x} u_g + \frac{\partial \xi}{\partial y} v_g \tag{5}$$

$$V_g = \frac{\partial \eta}{\partial x} u_g + \frac{\partial \eta}{\partial y} v_g \tag{6}$$

where, depth averaged seepage flow velocities along x and y coordinates in Cartesian coordinate system are shown as u_g, v_g, respectively. Λ is a parameter related to the porosity in the soil, wherein Λ = 1 as $z \gamma z_b$, and $\Lambda = \lambda$ as $z < z_b$, where z_b is the bed level and λ is the porosity in the soil. Seepage flow is assumed as horizontal two-dimensional saturation flow. Momentum equations of surface water are as follows.

$$\begin{aligned}
&\frac{\partial}{\partial t}\left(\frac{hU}{J}\right)+\frac{\partial}{\partial \xi}\left(U\frac{hU}{J}\right)+\frac{\partial}{\partial \eta}\left(V\frac{hU}{J}\right)\\
&-\frac{hu}{J}\left(\frac{\partial}{\partial t}\left(\frac{\partial \xi}{\partial x}\right)+U\frac{\partial}{\partial \xi}\left(\frac{\partial \xi}{\partial x}\right)+V\frac{\partial}{\partial \eta}\left(\frac{\partial \xi}{\partial x}\right)\right)\\
&-\frac{hv}{J}\left(\frac{\partial}{\partial t}\left(\frac{\partial \xi}{\partial y}\right)+U\frac{\partial}{\partial \xi}\left(\frac{\partial \xi}{\partial y}\right)+V\frac{\partial}{\partial \eta}\left(\frac{\partial \xi}{\partial y}\right)\right)\\
&=-gh\left(\frac{1}{J}\left(\left(\frac{\partial \xi}{\partial x}\right)^2+\left(\frac{\partial \xi}{\partial y}\right)^2\right)\frac{\partial z_s}{\partial \xi}+\frac{1}{J}\left(\frac{\partial \xi}{\partial x}\frac{\partial \eta}{\partial x}+\frac{\partial \xi}{\partial y}\frac{\partial \eta}{\partial y}\right)\frac{\partial z_s}{\partial \eta}\right)-\frac{\tau_{b\xi}}{\rho J}\\
&+\frac{1}{J}\left(\frac{\partial \xi}{\partial x}\right)^2\frac{\partial}{\partial \xi}(h\sigma_{xx})+\frac{1}{J}\frac{\partial \xi}{\partial x}\frac{\partial \eta}{\partial x}\frac{\partial}{\partial \eta}(h\sigma_{xx})+\frac{1}{J}\frac{\partial \xi}{\partial y}\frac{\partial \eta}{\partial x}\frac{\partial}{\partial \eta}(h\tau_{yx})+\frac{1}{J}\frac{\partial \xi}{\partial y}\frac{\partial \xi}{\partial x}\frac{\partial}{\partial \xi}(h\tau_{yx})\\
&+\frac{1}{J}\frac{\partial \xi}{\partial x}\frac{\partial \eta}{\partial y}\frac{\partial}{\partial \eta}(h\tau_{xy})+\frac{1}{J}\frac{\partial \xi}{\partial x}\frac{\partial \xi}{\partial y}\frac{\partial}{\partial \xi}(h\tau_{xy})+\frac{1}{J}\left(\frac{\partial \xi}{\partial y}\right)^2\frac{\partial}{\partial \xi}(h\sigma_{yy})+\frac{1}{J}\frac{\partial \xi}{\partial y}\frac{\partial \eta}{\partial y}\frac{\partial}{\partial \eta}(h\sigma_{yy})
\end{aligned} \tag{7}$$

$$\begin{aligned}
&\frac{\partial}{\partial t}\left(\frac{hV}{J}\right)+\frac{\partial}{\partial \xi}\left(U\frac{hV}{J}\right)+\frac{\partial}{\partial \eta}\left(V\frac{hV}{J}\right)\\
&-\frac{hu}{J}\left(\frac{\partial}{\partial t}\left(\frac{\partial \eta}{\partial x}\right)+U\frac{\partial}{\partial \xi}\left(\frac{\partial \eta}{\partial x}\right)+V\frac{\partial}{\partial \eta}\left(\frac{\partial \eta}{\partial x}\right)\right)\\
&-\frac{hv}{J}\left(\frac{\partial}{\partial t}\left(\frac{\partial \eta}{\partial y}\right)+U\frac{\partial}{\partial \xi}\left(\frac{\partial \eta}{\partial y}\right)+V\frac{\partial}{\partial \eta}\left(\frac{\partial \eta}{\partial y}\right)\right)\\
&=-gh\left(\frac{1}{J}\left(\frac{\partial \xi}{\partial x}\frac{\partial \eta}{\partial x}+\frac{\partial \xi}{\partial y}\frac{\partial \eta}{\partial y}\right)\frac{\partial z_s}{\partial \xi}+\frac{1}{J}\left(\left(\frac{\partial \eta}{\partial x}\right)^2+\left(\frac{\partial \eta}{\partial y}\right)^2\right)\frac{\partial z_s}{\partial \eta}\right)-\frac{\tau_{b\eta}}{\rho J}\\
&+\frac{1}{J}\frac{\partial \eta}{\partial x}\frac{\partial \xi}{\partial x}\frac{\partial}{\partial \xi}(h\sigma_{xx})+\frac{1}{J}\left(\frac{\partial \eta}{\partial x}\right)^2\frac{\partial}{\partial \eta}(h\sigma_{xx})+\frac{1}{J}\frac{\partial \eta}{\partial y}\frac{\partial \xi}{\partial x}\frac{\partial}{\partial \xi}(h\tau_{yx})+\frac{1}{J}\frac{\partial \eta}{\partial y}\frac{\partial \eta}{\partial x}\frac{\partial}{\partial \eta}(h\tau_{yx})\\
&+\frac{1}{J}\frac{\partial \eta}{\partial x}\frac{\partial \xi}{\partial y}\frac{\partial}{\partial \xi}(h\tau_{xy})+\frac{1}{J}\frac{\partial \eta}{\partial x}\frac{\partial \eta}{\partial y}\frac{\partial}{\partial \eta}(h\tau_{xy})+\frac{1}{J}\frac{\partial \eta}{\partial y}\frac{\partial \xi}{\partial y}\frac{\partial}{\partial \xi}(h\sigma_{yy})+\frac{1}{J}\left(\frac{\partial \eta}{\partial y}\right)^2\frac{\partial}{\partial \eta}(h\sigma_{yy})
\end{aligned} \tag{8}$$

Where, g is the gravity, ρ is the water density. $\tau_{b\xi}$ and $\tau_{b\eta}$ represent the contravariant shear stress along ξ and η coordinates, respectively. These shear stresses are defined as

$$\tau_{b\xi} = \frac{\partial \xi}{\partial x}\tau_{bx} + \frac{\partial \xi}{\partial y}\tau_{by} \tag{9}$$

$$\tau_{b\eta} = \frac{\partial \eta}{\partial x}\tau_{bx} + \frac{\partial \eta}{\partial y}\tau_{by} \tag{10}$$

where, τ_x and τ_y are the shear stress along x and y coordinates, respectively as follows.

$$\tau_x = \tau_b \frac{u_b}{\sqrt{u_b^2 + v_b^2}} \tag{11}$$

$$\tau_y = \tau_b \frac{v_b}{\sqrt{u_b^2 + v_b^2}} \tag{12}$$

$$\frac{\tau_b}{\rho} = u_*^2 \tag{13}$$

$$u_*^2 = \frac{n_m^2 g}{R^{1/3}}\left(u^2 + v^2\right) \tag{14}$$

Where, u_* is the friction velocity, n_m is the Manning's roughness coefficient, R is the hydraulic radius, k_s is the roughness height. u_b and v_b represent velocity near the bed surface along x and y coordinates, respectively. Velocities near the bed are evaluated using curvature radius of streamlines as follows.

$$u_b = u_{bs}\cos\alpha_s - v_{bs}\sin\alpha_s \tag{15}$$

$$v_b = u_{bs}\sin\alpha_s + v_{bs}\cos\alpha_s \tag{16}$$

$$u_{bs} = 8.5u_* \tag{17}$$

$$v_{bs} = -N_* \frac{h}{r} u_{bs} \tag{18}$$

Where, $\alpha_s = \arctan(v/u)$, N_* is 7.0 (Engelund, 1974) and r is the curvature radius of stream lines obtained by depth integrated velocity field as follows (Shimizu and Itakura, 1991).

$$\frac{1}{r} = \frac{1}{\left(u^2+v^2\right)^{3/2}}\left\{u\left(u\frac{\partial v}{\partial x} - v\frac{\partial u}{\partial x}\right) + v\left(u\frac{\partial v}{\partial y} - v\frac{\partial u}{\partial y}\right)\right\} \tag{19}$$

σ_{xx}, σ_{yy}, τ_{xy} and τ_{yx} are turbulence stresses as follows.

$$\sigma_{xx} = 2\nu \frac{\partial u}{\partial x} \tag{20}$$

$$\sigma_{yy} = 2\nu \frac{\partial v}{\partial y} \tag{21}$$

$$\tau_{xy} = \tau_{yx} = \nu \left(\frac{\partial v}{\partial x} + \frac{\partial u}{\partial y} \right) \tag{22}$$

$$\nu = \frac{\kappa}{6} u_* h \tag{23}$$

Where, ν is the coefficient of kinematics eddy viscosity, κ is the Karman constant, k_t is the depth-averaged turbulence kinetic energy (Takebayashi, 2005).

$$u_g = -k_{gx} \left(\frac{\partial \xi}{\partial x} \frac{\partial z_b}{\partial \xi} + \frac{\partial \eta}{\partial x} \frac{\partial z_b}{\partial \eta} \right) \tag{24}$$

$$v_g = -k_{gy} \left(\frac{\partial \xi}{\partial y} \frac{\partial z_b}{\partial \xi} + \frac{\partial \eta}{\partial y} \frac{\partial z_b}{\partial \eta} \right) \tag{25}$$

Where, k_{gx} and k_{gy} is the coefficient of permeability along the longitudinal and the transverse directions, respectively. When the water depth of surface flow becomes less than the mean diameter of the bed material, the surface flow is computed only in consideration of the pressure term and bed shear stress term in the momentum equation of surface flow (Nagata, 1999).

4. Results and Discussions

Flow pattern and deformation of the bed near the bank toe as important parameters on triggered the initial bank erosion process (Simon et al., 2000). The flow pattern and the deformation of bed near the bank, especially during low stages are discussed. This condition may produce high energy due to the different water level between upstream and downstream.

Simulation cases are Case 1a, Case 1d, Case 2a and Case 2d. Case 1a is the original condition. The bed geometry of the original condition is measured in 2008. Case 1d is the simulation considering the dredging of the mid channel bar. The bed material higher than +21.00 m is removed in Case 1d. Case 2a is the simulation considering the structure of preventing bank erosion. In this case, the revetment is installed along the bank, where the bank was collapsed. Case 2d is the simulation considering combination methods in Case 1d and Case 2a. The dredging location is shown in Fig. 5 at B area. The location of revetment is shown in Fig. 5 (b) indicated by two arrows at the start and end point. Bed deformations near the bank toe are investigated at cross section C3 as shown in Fig. 5.

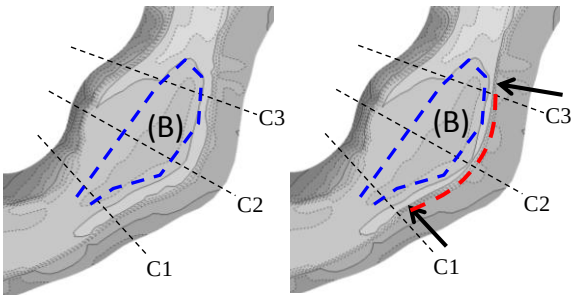

(a) (b)

Fig. 5 Topography of the study reach used for the simulations

Fig. 6, 7, 8 and 9 show the horizontal distributions of velocity vector under the lowest water surface level condition at the downstream area. The small size of the vector indicates the low velocity and the big size indicates the high velocity.

In Case 1a (see Fig. 6), the flow divided into two parts by the presence of the mid channel bar and produce high and convergence velocity at lee area (the downstream of the bar which is indicated by the blue circle). This may become a strong reason that bank erosion occurred there. However, after the mid channel bar was dredged (see Fig. 7, Case 1d), the flow velocity in this area decreases significantly. This means that the dredging method can control the flow velocity near the bank. In Fig. 8, the flow velocity around lee area still has high magnitude. And also tend to increase the flow velocity at the opposite side as indicated by the red circle. In this area, the flow velocity will decrease significantly after the dredging of the mid channel bar (see Fig. 9). These results show that the horizontal distribution of velocity on Case 2a and Case 2d are similar. Its means that the revetment seems unnecessary as a countermeasure of the bank erosion problem in this river each.

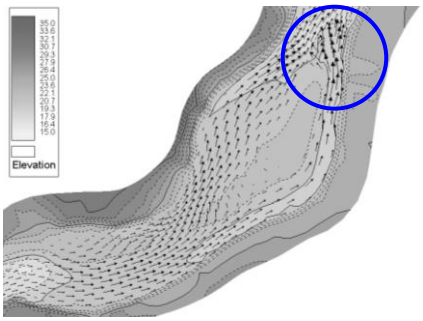

Fig. 6 Horizontal distribution of flow velocity in Case 1a

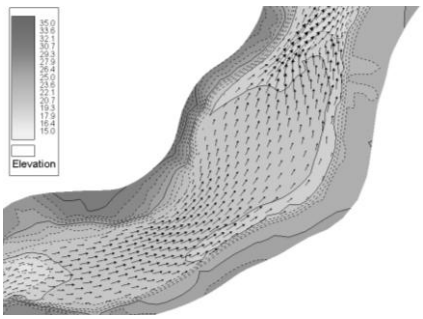

Fig. 7 Horizontal distribution of flow velocity in Case 1d

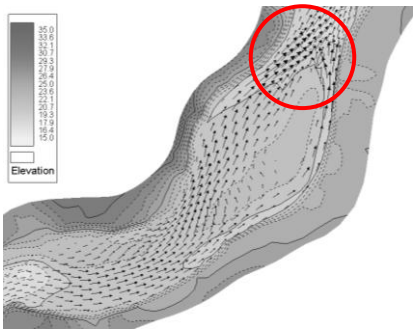

Fig. 8 Horizontal distribution of flow velocity in Case 2a

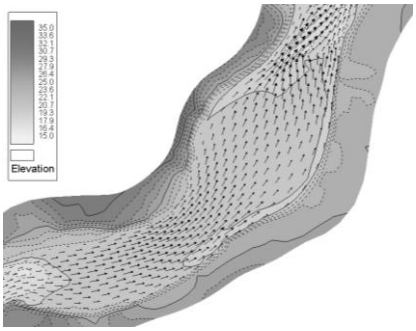

Fig. 9 Horizontal distribution of flow velocity in Case 2d

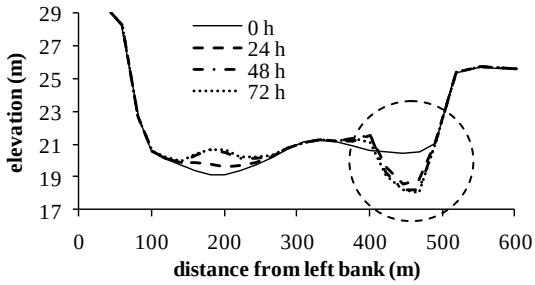

Fig. 10 Cross section profile C3 in Case 1a

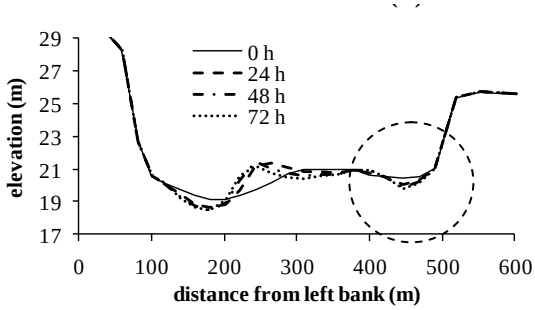

Fig. 11 Cross section profile C3 in Case 1d

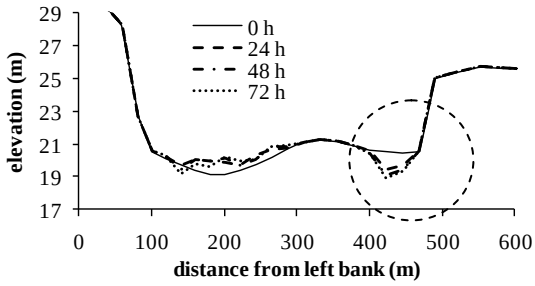

Fig. 12 Cross section profile C3 in Case 2a

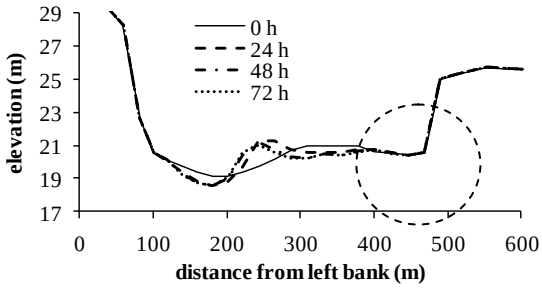

Fig. 13 Cross section profile C3 in Case 2d

Furthermore, the effect of the dredging and installing revetment will be discussed considering on the erosion rate at the bank toe. Fig. 10, 11, 12 and 13 is the cross section at C3 for Case 1a, Case 1d, Case 2a and Case 2d, respectively. In Case 1a, the bed near the bank toe (at right bank) was eroded more. By the dredging of the mid channel bar in

Case 1d, the bed degradation is reduced significantly. In Case 2a, the bed degradations still occur more in spite of the installation of revetment. Its means that after installing the revetment, the bed degradations near the bank toe still occurs, and will affect on the stability of the structure. However, after dredging of the mid channel bar (Case 2d), the bed degradation reduces significantly. This condition is similar with Case 1a. By considering the cost of the structure of revetment, it seems that this structure is not unnecessary.

5. Conclusions

The horizontal two-dimensional bed deformation analysis is applied to the Sesayap River. Furthermore, the advantage of the dredging is discussed. The dredging of the mid channel bar is the appropriate choice for the countermeasure of the bank erosion problem in Sesayap River reach at Malinau, when the financial efficiency, bed degradation along both banks and the horizontal distribution of velocity in the lee area are considered.

Acknowledgements

Many thanks are given to Prof. Djoko Legono, Dr. Faisal Fathani, Ir. Suyitno, MT., Mr. Ade and all members of the Hydraulics Studio of Gadjah Mada University that given to the author encouragement and gratefully support during the field survey in Sesayap River. Many thanks also are given to Malinau Distric Government.

References

Thorne, C.R. (1991): Bank Erosion and Meander Migration of The Red and Mississippi Rivers, USA, Proceedings of the Vienna Symposium, IAHS, Publ. no. 201.

Schumm S.A. (1985): Patterns of Alluvial Rivers, Ann. Rev. Earth Planet. Sci., Vol. 13, pp. 5-27.

Brierly G.J., and Fryirs K.A. (2005): Geomorphology and River Management, Application of the River Styles Framework, Blackwell Publishing.

Dulal K.P., and Shimizu Y (2010): Experimental Simulation of Meandering in Clay Mixed Sediment, Journal of Hydro-environment Research, Vol. 20, pp. 1-15.

Takebayashi H, Fujita M, and Harsanto P. (2010): Numerical Analysis of Bank Erosion Process Along Banks Composed of Both Cohesive and Non-Cohesive Layers, International Workshop on Multimodal Sediment Disasters Triggered by Heavy Rainfall and Earthquake and the Countermeasures, Vol. 1.

Takebayashi, H. (2005): River Configuration in Middle-Lower Reach of River Basin, Journal of Japan Society of Fluid Mechanics, Vol. 24, pp. 27-36.

Engelund, F. (1974): Flow and Bed Topography in Channel Bends, Journal of Hydraulic Div., ASCE, Vol. 100, No. HY11.

Shimizu,Y. and Itakura,T. (1991): Calculation of Flow and Bed Deformation with a General Non-Orthogonal Coordinate System, Proc. of XXIV IAHR Congress, Spain, C-2, pp.41-48.

Nagata, N. (1999): Numerical Analysis of the 2-Dimensional Unsteady Flow Using a Generalized Coordinate System, The Lecture Collection on the Computer Use in Hydraulic Engineering, The Japan Society of Civil Engineers, pp. 51 – 76.

Simon A., Curini A., Darby S.E., and Langendoen E.J. (2000): Bank and near-bank processes in an incised channel, Geomorphology, Vol. 35, pp. 193-217.

(Received June 7, 2012)

セサヤップ川における河岸浸食対策に関する数値解析

Puji HARSANTO[1]・竹林洋史・藤田正治

[1]京都大学大学院工学研究科

要　旨

本稿は，河川域における平面二次元の流れと河床変動特性を考慮した河岸浸食対策法について扱っている．数値解析では，一般座標系で記述しされた平面二次元河床変動解析の基礎方程式を用いて行われた．河川領域内の中州の存在は，河岸浸食を発生させる一つの要因となっていることが解析結果より明らかとなった．また，適度な中州の掘削によって河岸浸食が抑制されることが明らかとなった．さらに，護岸の建設は対象とした河岸を守ることは可能であるが，対岸への流れを速やかにするため，対岸での河岸付近の局所洗掘を助長する場合がある．

キーワード:河岸浸食，中州，数値解析，河床変動